Pergamon

Cement and Concrete Research, Vol. 25, No. 8, pp. 1605-1609, 1995

0008-8846/95 $9.50+.00

0008-8846(95)00154-9

COMMUNICATED PAPERS

THE ELASTIC MODULI OF CALCIUM HYDROXIDE

Paulo J.M. Monteiro and C. T. Chang
Department of Civil Engineering
University of California
Berkeley, CA 94720

(Communicated by J.P. Skalny)
(Received August 7, 1995)

New sophisticated micromechanical theories based on the mathematical morphology of concrete can improve significantly the modeling of concrete. To fully utilize these models, it is necessary to determine the intrinsic properties of the cement paste hydration products. At present, there is only limited information on the elastic moduli of portland cement components and hydration products, such as calcium silicate hydrated, calcium hydroxide, ettringite, and monosulfate hydrated. This note reviews (a) the elastic stiffness coefficients of calcium hydroxide, (b) analyzes the corresponding Reuss, Voigt and Hashin-Shtrikman (H-S) bounds, and (c) suggests values to be used in the micromechanical models.

The determination of the elastic moduli of calcium hydroxide is difficult because large single crystals without flaws are not available. To circumvent this limitation, research has been performed using the Brillouin spectrum (1), compressing small crystals in a diamond cell (2), and testing compacted powder samples of different porosities (3,4). Table 1 shows the elastic stiffness coefficients of calcium hydroxide as determined by the Brillouin spectrum (1).

TABLE 1
Elastic Stiffness Coefficients of Calcium Hydroxide (10^{10} N/m^2)

c_{11} = 9.928	c_{33} = 3.26
c_{12} =3.618	c_{44} = 0.9846
c_{13} = 2.965	c_{66} = 3.155

Most micromechanical models dealing with the microstructure of cement paste require macroscopic averaging of the elastic moduli, rather than the properties of the single crystal. The homogenization equations proposed by Voigt and Reuss for crystals of hexagonal symmetry are given in Table 2 (5,6).

TABLE 2

Voigt bounds	Reuss bounds
$K_v = \frac{1}{9}\left[2(c_{11}+c_{12}) + c_{33} + 4c_{13}\right]$	$K_r = \frac{c^2}{M}$
$G_v = \frac{1}{30}\left(M + 12c_{44} + 12c_{66}\right)$	$G_r = \frac{5}{2}\frac{c^2 c_{44} c_{66}}{3K_v c_{44} c_{66} + c^2(c_{44} + c_{66})}$

where

$M = c_{11} + c_{12} + 2c_{33} - 4c_{13}$ and $c^2 = (c_{11} + c_{12})c_{13} - 2c_{13}^2$

The results for the Voigt and Reuss models are presented in Table 4. Hill (6) showed that the Voigt and Reuss equations lead to the upper and lower bounds on the effective elastic moduli, respectively. The arithmetic mean of the Voigt and Reuss bounds is often referred to as the Voigt-Reuss-Hill (VRH) average and, often, it can provide an adequate approximation for the elastic moduli. It is possible to narrow the Voigt and Reuss bounds on the elastic moduli of hexagonal crystals by applying the variational principles developed by Hashin and Shtrikman (7). Their approach gives the best bounds on the elastic moduli for polycrystals without making any assumption on the geometry or the crystal orientation within the polycrystal. The following equations are used to obtain the upper and lower bounds for K and G (8, 9):

$$K_{HS} \lesseqgtr K_o + \frac{(K_v - K_o) - \frac{1}{3}\beta\Delta}{1 - \frac{1}{3}\beta(M - 6G_o)} \quad (1)$$

$$G_{HS} \lesseqgtr G_o + \frac{A}{1 + 2\beta A} \quad (2)$$

where,

$$\alpha = -\frac{3}{3K_o + 4G_o} \quad (3)$$

$$\beta = -\frac{3(K_o + 2G_o)}{5G_o(3K_o + 4G_o)} \quad (4)$$

$$\gamma = \frac{1}{9}(\alpha - 3\beta) \quad (5)$$

$$30A = \frac{M - 6G_o - \alpha\Delta}{1 - \beta(c_{11} + c_{12} + c_{33} - 3K_o - 2G_o) - 9\gamma(K_v - K_o) + \frac{1}{3}\alpha\beta\Delta} + \frac{12(c_{44} - G_o)}{1 - 2\beta(c_{44} - G_o)} + \frac{12(c_{66} - G_o)}{1 - 2\beta(c_{66} - G_o)} \quad (6)$$

$$\Delta = c^2 - K_o(M - 6G_o) - 6G_o K_v \quad (7)$$

The bounds are determined once the values for K_o and G_o are computed. Figure 1 indicates the positive and negative regions in the K_o and G_o plane for calcium hydroxide. The expressions for the negative and positive definite boundaries are given in Table 3.

TABLE 3

$K_o = c_{11} - \frac{4}{3}G_o$ (8)	$K_o = \frac{(c^2 - 6K_v G_o)}{(M - 6G_o)}$ (10)	$G_o = c_{66}$ (12)
$K_o = \frac{1}{2}(c_{11} + c_{12}) - \frac{1}{3}G_o$ (9)	$G_o = c_{44}$ (11)	

The values for K_o and G_o, which give the greatest lower bounds, were determined (8,9) and the H-S bounds for bulk and shear moduli for calcium hydroxide are given in Table 4.

The upper (or lower) bound on the Young's modulus, *E*, and on the Poisson's ratio, ν, can be determined by placing the H-S upper (or lower) bounds on *K* and *G* into the relationships (10):

$$\frac{9K_L G_L}{3K_L + G_L} \leq E \leq \frac{9K_U G_U}{3K_U + G_U} \quad (8)$$

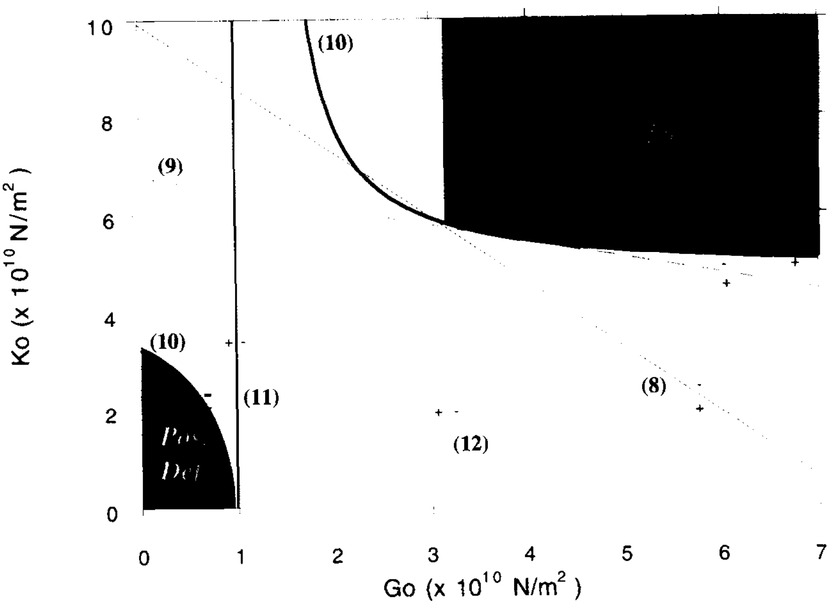

FIG. 1

Positive and negative definite regions for calcium hydroxide using equations 8-12

TABLE 4

Elastic Moduli of Calcium Hydroxide (10^{10} N/m^2)

	Voigt	*Reuss*	HS_L	HS_U	*VRH*
Bulk Modulus	4.690	3.239	3.781	4.271	3.965
Shear Modulus	1.929	1.347	1.501	1.694	1.636

where, $VRH = (Voigt + Reuss)/2$ (9)

$$\frac{3K_L - 2G_U}{6K_L + 2G_U} \leq \nu \leq \frac{3K_U - 2G_L}{6K_U + 2G_L} \tag{9}$$

The range for Young's modulus is 3.977 to 4.489 10^{10} N/m^2 and for Poisson's ratio is 0.305 to 0.343.

Meade and Jeanloz (2) performed X-ray diffraction measurements on calcium hydroxide as it was compressed in a diamond cell at room temperature. The static compression test provided direct measurements of the bulk modulus and the linear incompressibilities along the unit cell axes. Their experimental value for bulk modulus of 3.78 (± 0.18) 10^{10} N/m^2 lies on the lower H-S bound. They observed that the *c* direction is approximately three times as compressible as the *a* direction due to the differences in bonding along the *a* and *c* directions. The OH ··· O bonds in the *c* direction are much more compressible than the Ca-O bond in the *a* direction.

Taking the experimental result of Meade and Jeanloz as $K = K_{exp}$, it is possible to further reduce the bounds for the remaining elastic moduli. Because E is an increasing function of G for any fixed value of K, the smallest possible value of E would occur if $G = G_L$ and the largest possible value of E would occur if $G = G_U$:

$$\frac{9\,K_{exp}\,G_L}{3\,K_{exp} + G_L} \leq E \leq \frac{9\,K_{exp}\,G_U}{3\,K_{exp} + G_U} \tag{10}$$

The bounds given in equation 10 are superior to those given in equation 8. The range reduces to 3.977 and 4.422 10^{10} N/m^2. This can be seen in Fig. 2 where the H-S bounds on the $\{G,K\}$ plane are a rectangle (11), restricting E to be between $E = E_L$ and $E = E_U$. Taking $K = K_{exp}$, the rectangle reduces to a horizontal line in the $\{G,K\}$ plane, restricting E to be between E_1 and E_2, which are given in equation (10). Since the experimental value for bulk modulus (K_{exp}) lies on the lower H-S bound, $E_1 = E_L$. The new bounds are tighter than the H-S bounds. Similarly, tighter bounds can be obtained for Poisson's ratio by introducing the value of $K = K_{exp}$ into equation 9, leading to $0.305 \leq \nu \leq 0.325$.

Figure 3 shows the results from compacted samples of calcium hydroxide of different porosities (3,4). Wittmann (3) and Beaudoin (4) estimated Young's modulus at zero porosity to be 4.8 and 3.52 10^{10} N/m^2, respectively. These values are outside the H-S bounds. Both researchers obtained the extrapolation to zero porosity by assuming a linear relationship between porosity and the logarithm of Young's modulus; there is, however, no theoretical basis for assuming such a relationship. One possible explanation for the significant differences in the experimental results of Wittmann and Beaudoin could be that pores with different aspect ratios were created during the manufacturing of the compacted samples. It is well known that pore geometry play a very important role in determining the elastic moduli of a porous medium (12-13). This analysis emphasizes the importance for the H-S bounds and recommends that in future work using compacted samples, both the total porosity and a geometrical description of the pores should be included, so that powerful models such as the differential scheme or the modified self-consistent method, could be used to predict Young's modulus at zero porosity.

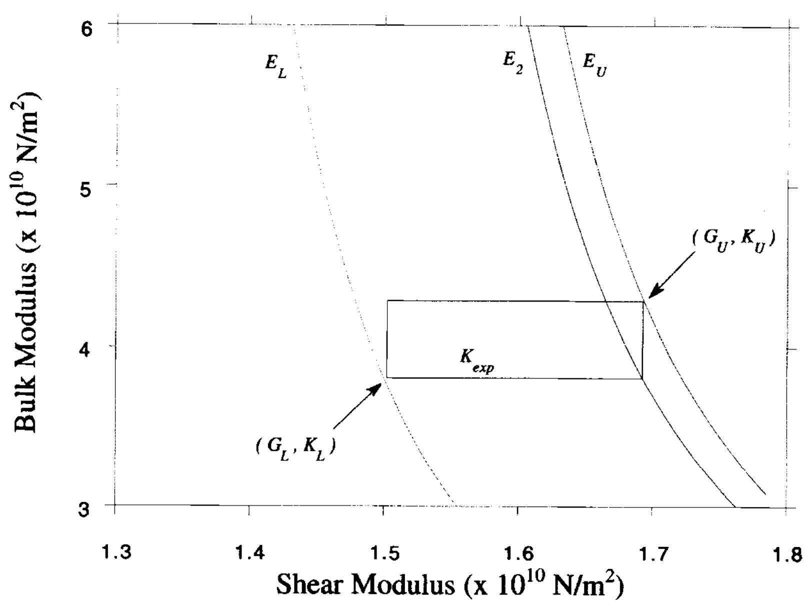

FIG. 2

Bounds on Young's Modulus on the $\{G, K\}$ plane

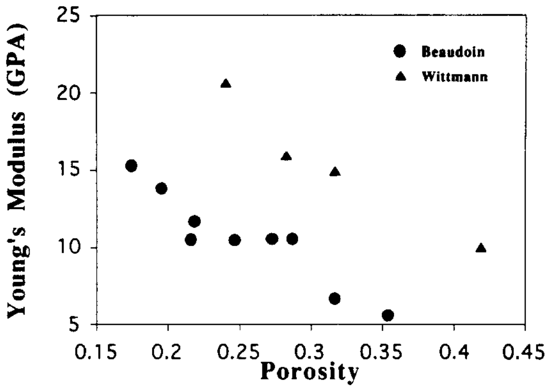

FIG. 3
Young's modulus of calcium hydroxide compacts as a function of porosity

Acknowledgments

The authors wish to thank Dr. R. Zimmerman for his insightful comments.

References

1. F. Holuj, M. Drozdowski and M. Czajkowski, Solid State Comunications, 56, 1019 (1985).
2. C. Meade and R. Jeanloz, Geophysical Research Letters, Geophysical Research Letters, 17, 1157 (1990).
3. F.H. Wittmann, Cement and Concrete Research, 16, 971 (1986).
4. J.J. Beaudoin, Cement and Concrete Research, 13, 319 (1983).
5. M. J. P. Musgrave, *Crystal Acoustics*, Holden-Day, Inc, San Francisco (1970).
6. R. Hill, Proceedings of the Physical Society of London, 65A, 349 (1952).
7. Z. Hashin and S. Shtrikman, J. Mech. Phys. Solids, 11, 127 (1963).
8. J.P. Watt and L. Peselnick, J. Appl. Phys., 51, 1525, (1980).
9. L. Peselnick and R. Meister, J. Appl. Phys., 36, 2879 (1965).
10. R. Zimmerman, Mechanics Research Communications, 19, 563 (1992).
11. J.G. Beryman and G. W. Milton, J. Phys. D: Appl. Phys. 21, 87 (1988).
12. R. M. Christensen, Proc. R. Soc. Lond. A, 440, 461 (1993).
13. R. W. Zimmerman, Mechanics of Materials, 12, 17 (1991).